PLANETARY NEBULAE AS A TOOL FOR STUDY STELLAR EVOLUTION

K. Gesicki[1], A. A. Zijlstra[2], A. Acker[3]

[1]Centrum Astronomii UMK,
ul. Gagarina 11, PL-87-100 Torun, Poland

[2]School of Physics and Astronomy, University of Manchester
P.O. Box 88, Manchester M60 1QD, UK

[3]Observatoire astronomique de Strasbourg,
11 rue de l'Universite, 67000 Strasbourg, France

During years of photoionization and kinematic modelling we collected a sample of data for 101 planetary nebulae. We present three aspects of using these data for study stellar evolution:

- We have uniform estimations of central stars effective temperatures. We assemble the histograms of $T_{\rm eff}$ distribution and compare them with those derived from Blöcker (1995) tracks.
- We have uniform estimations of the nebular dynamical ages. Assuming that they correspond to the true ages we compare them with time sequences of Blöcker(1995).
- The three best studied objects are compared to recent hydrodynamical computations of nebular evolution. This reveals problems concerning an important evolutionary phase – the transition between AGB superwind and post-AGB fast wind.

1 METHODS

We derive information on the nebula using a combination of line ratios, diameters, and high resolution spectra. The models find the density distribution, stellar temperature and the velocity field.

- The diameters and line ratios are used to fit a photo-ionization model.
- The model is constrained to reproduce the intensity distribution of images, if any are available.
- The stellar temperature assumes a black-body spectrum energy distribution – therefore we rather call it $T_{\mathrm{b-b}}$ than T_{eff}. Although this assumption can be challenged, it has the advantage of providing a uniform measure of the temperature over a range of stellar classes.
- Line profiles are obtained from the high resolution spectra, and are fitted using the emissivity distributions of the photoionization model, and assuming a velocity field.
- The velocity fields include separate contributions from expansion and turbulence. Turbulence always includes the instrumental broadening and the thermal broadening (calculated from the photoionization model), but some objects require additional turbulence.
- We define the expansion velocity as a mass-weighted average over the nebula, V_{av}. This parameter has been shown to be robust: it can be accurately determined even when the velocity field itself is uncertain. This allows us to define a kinematic age to the nebula. We make corrections for the expected acceleration of the nebula after the onset of the ionization.

The full analyzed sample of 101 PNe contains 23 [WR]-type, 21 *wels* (weak emission line stars) and 57 non-emission-line central stars.

2 TEMPERATURE DISTRIBUTIONS

We compare the temperature distribution of the various PNe samples with that predicted by the evolutionary tracks.

We interpolated the tracks, to calculate the predicted number of stars per temperature range (as proportional to the time spent in the range). The histogram concerns only the horizontal part of the evolutionary track before the turn-off in the H-R diagram. Dotted line in Fig. 1 shows the predicted distributions for hydrogen burning $0.605\mathrm{M}_{\odot}$ track of Blöcker (1995).

UPPER PANEL

Summing both types of emission-line stars, i.e. [WR] and *wels*, we obtained a flat distribution.

CENTRAL PANEL

The non-emission-line cores show an excess at about 100 kK in comparison to the H-burning models and a deficit at even higher temperatures.

It is possible that for some reason our observations misrepresent the oldest PNe with the hottest cores. Note that our sample is mainly restricted to the spherical PNe with ionization boundary while for old PNe the ionization front breaks through and may cause fragmentation of a nebula making it not suitable for our analysis. We also cannot exclude a systematic error of our $T_{\mathrm{b-b}}$ values which may shift the maximum of the observed distribution.

BOTTOM PANEL

It is interesting to see that the best agreement is obtained for the sum of all PNe. Both emission and non-emission cores separately show different slopes than the gradually increasing theoretical histogram.

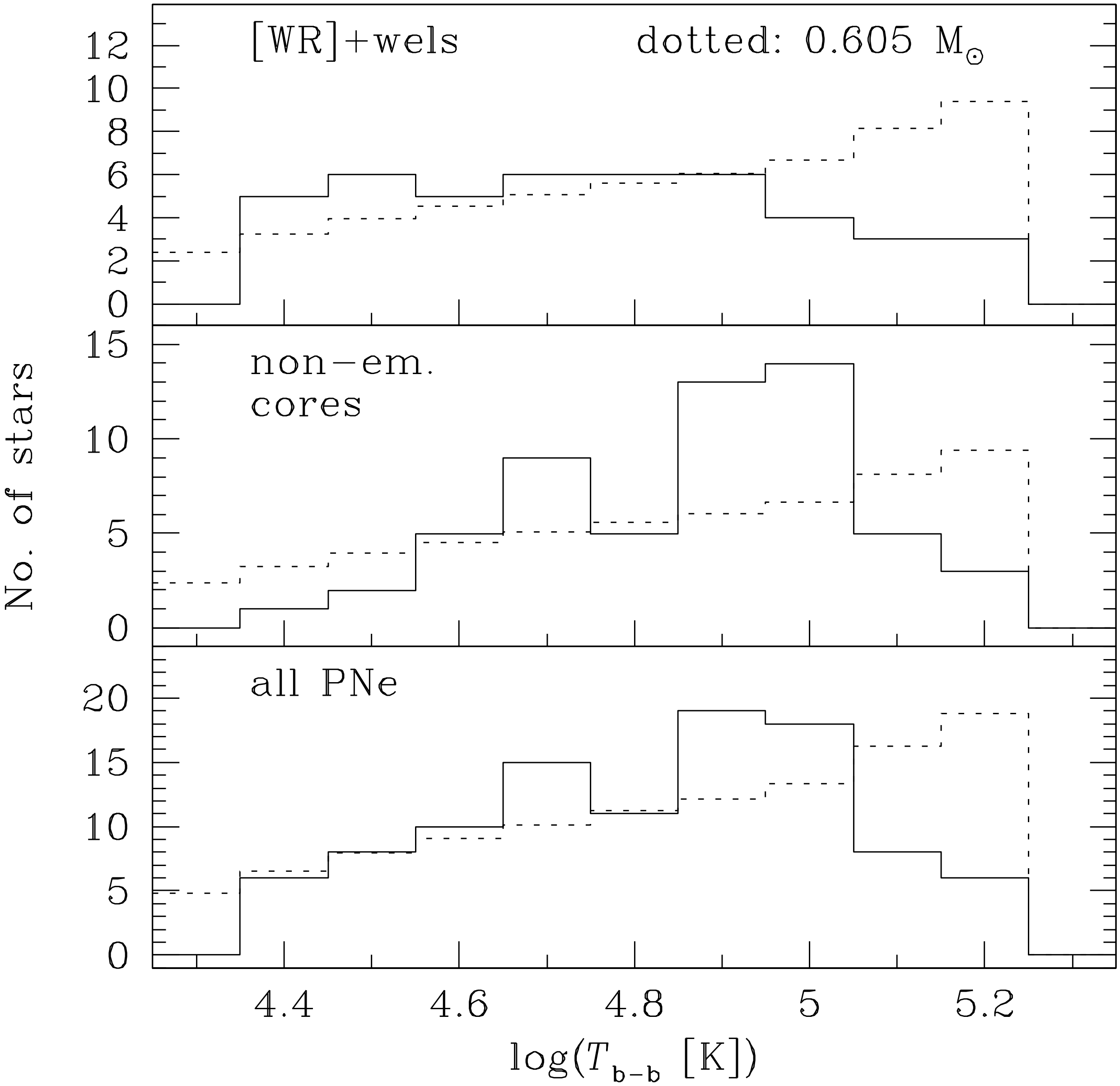

Figure 1: Temperature distribution of emission-line ([WR] and *wels*), non-emission-line stars, and the whole sample, in logarithmic temperature bins. The dotted line shows histograms obtained from H-burning evolutionary models of Blöcker.

3 DYNAMICAL AGES

The expansion velocity and radius of the nebula can be used to derive the age of the nebula. We apply the mass-averaged velocity, and use for the radius 0.8 of the outer radius, roughly corresponding to the mass-averaged radius. To account for the acceleration of the nebula we average between the current velocity and that of the original outflow velocities on the Asymptotic Giant Branch. We made a simplified assumption about the AGB outflow velocity setting it equal to $10\,\mathrm{km\,s^{-1}}$ for all objects.

Fig. 2 plots the dynamical age versus the temperature for the stars in our sample. The interpolated (hydrogen-burning) evolutionary tracks are overplotted with a solid line. Different symbols distinguish types of stars and indicate turbulence.

The figure shows that some regions in this age-temperature plane are dominated by certain types of objects.

- The [WR] stars are mainly found in the narrow region between the 0.605 and $0.625\,\mathrm{M_\odot}$ tracks, with a few further objects at low temperatures and a range of ages.
- The *wels* stars are spread out at intermediate temperatures.
- The non-emission-line stars tend to avoid the low temperature region, but cover a region in the top-right corner which the other stars avoid.

Among the coolest stars, the population is strongly dominated by [WC] stars. It is surprising how few non-emission-line stars are found in this region.

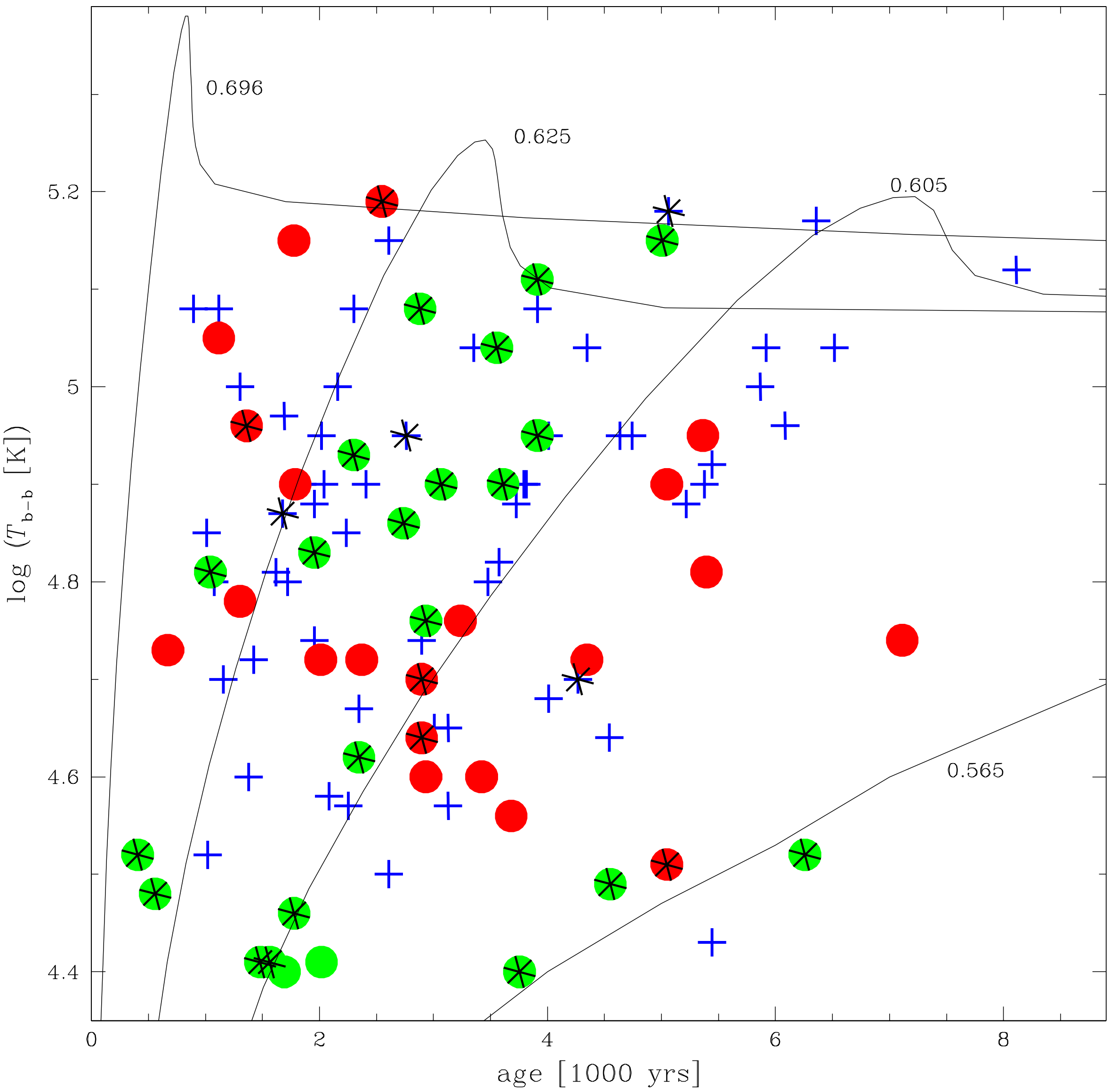

Figure 2: The age–temperature diagram. Green circles indicate [WR] stars, red circles are *wels* and pluses indicate non-emission-line stars. Turbulent nebulae are indicated by the star symbols. Solid lines show Schönberner's H-burning evolution.

4 OBSERVED DENSITY STRUCTURES

In Gesicki & Zijlstra (2003, MNRAS 338, 347) we analyzed deep echelle spectra from three nebulae in the Bulge, the Sagittarius Dwarf and the SMC. These have the advantage that the distances are approximately known, which benefits the photo-ionization modeling. Diameters are known from published monochromatic images for all three nebulae. For the analysis we selected several (8–9) strong and well exposed lines which cover a broad range of excitation potentials. This allows us to probe the whole nebular depth. The SMC PN was unresolved but the other two PNe show line splitting in the low-excitation lines, which indicates they are partially resolved. We repeat here a fragment of the discussion from that paper, it is still relevant.

In our PNe, the inner cavity radius is about 10% of the outer shell radius. In the hydrodynamical models the inner radius of ionized nebula is about 50% of the outer radius. This difference suggests that the transition from AGB to post-AGB wind occurred different from Schönberner's scenario. We suggested that the fast wind may have been weaker than assumed in the hydrodynamical models. Alternatively, the star may have evolved faster (the core mass is slightly higher than in the models) giving the fast wind less time to act, or the AGB expansion velocity may have been low giving a denser, more compact AGB shell.

The structure of our PNe, with a high density inner ring and a low density outer region, corresponds to theoretical models $4-5\cdot10^3$ *years after the AGB. But the models are density bounded while our PNe are ionization bounded. Our PNe have inner rings denser and closer to the central star than the theoretical models. It is possible that the growing density of the inner shell blocked the ionizing radiation and a previously fully ionized PN entered a recombination phase.*